Contact Resistance with Dissimilar Materials: Bulk Contacts and Thin Film Contacts

Peng Zhang[1], Y. Y. Lau[1*], W. Tang[2], M. R. Gomez[3], D. M. French[2], J. C. Zier[4], and R. M. Gilgenbach[1]
[1]Department of Nuclear Engineering and Radiological Sciences
University of Michigan
Ann Arbor, USA
[2]Air Force Research Laboratory
Kirtland AFB, USA
[3] Sandia National Laboratories
Albuquerque, USA
[4]Naval Research Laboratory
Washington DC, USA

***Abstract*—Contact resistance is important to integrated circuits and thin film devices, carbon nanotube based cathodes and interconnects, field emitters, wire-array z-pinches, metal-insulator-vacuum junctions, and high power microwave sources, etc. In other applications, the electrical contacts are formed by thin film structures of a few microns thickness, such as in micro-electromechanical system (MEMS) relays and microconnector systems. This paper summarizes the recent modeling efforts at the University of Michigan, addressing the effect of dissimilar materials and of finite dimensions on the contact resistance of both bulk contacts and thin film contacts. The Cartesian and cylindrical geometries are analyzed. Accurate analytical scaling laws are constructed for the contact resistance of both bulk contacts and thin film contacts over a large range of aspect ratios and resistivity ratios. These were validated against known limiting cases and spot-checks with numerical simulations.**

Keywords- contact resistance; electrical contacts; contact potential; thin films; dissimilar materials; constriction resistance; spreading resistance

I. INTRODUCTION

Our interest in contact resistance was stimulated by the recognition of its importance in our ongoing studies of the Z-pinch [1], high power microwave generation [2], triple point junctions [3], field emitters [4], and heating phenomenology [5]. In learning the subject, we were always referred to the classical reference of Holm [6].

Holm's *a*-spot theory gives the electrical contact resistance of a circular constriction between two contacting surfaces as [6],

$$R = \frac{\rho}{4a} + \frac{\rho}{4a}, \tag{1}$$

where ρ is electrical resistivity and a is the contact spot radius. Implicit in the theory of Holm [6] are several assumptions: (A) the *a*-spot has a zero thickness, i.e., zero axial length in the direction of current flow, (B) the current channel is made of the same material, e. g., the effects of contaminants have been ignored, and (C) the contact members are bulk conductors, whose dimensions transverse to the current flow are infinite. Many subsequent models have been developed based on Holm's *a*-spot theory, adopting these three assumptions.

The *a*-spot theory has been extended by Timsit to include the effects of finite bulk radius [7, 8], thereby relaxing assumption (C). We have recently further extended the Holm-Timsit theory of *a*-spot by relaxing assumption (A), with the inclusion of a finite thickness in the contact "bridge" [9]. The scaling law developed in [9] was favorably tested against experiment [10]. We next included the effects of dissimilar materials [11], thereby *simultaneously* relaxing assumptions (A), (B), and (C) mentioned in the preceding paragraph. This generalized *a*-spot is shown in Fig. 1, where the resistivity ρ_1, ρ_2 and ρ_3, and the dimensions a, b, c, and h are arbitrary. In Section II, we present the scaling laws for the contact resistance in Fig. 1.

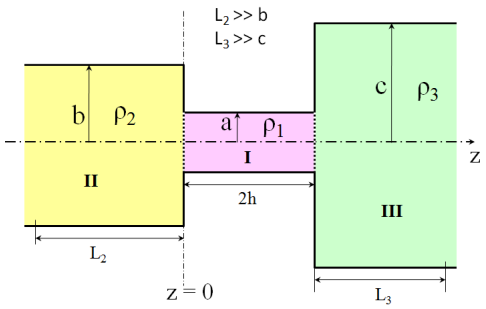

Figure 1. Two current channels, II and III, are made in contact through the bridge region, I, in either Cartesian or cylindrical geometries. Holm's *a*-spot corresponds to the cylindrical geometry with $h = 0$, $a << b$, $a << c$. Current flows from left to right.

For the thin film geometry shown in Fig. 2, we have also extended the traditional theory [12 - 16] to include the effects of dissimilar materials. This theoretical study was an adaptation

*Electronic mail: yylau@umich.edu

This work was supported by an AFOSR grant on the Basic Physics of Distributed Plasma Discharges, L-3 Communications Electron Device Division, and Northrop-Grumman Corporation. Two of us (PZ and DMF) gratefully acknowledge a fellowship from the University of Michigan Institute for Plasma Science and Engineering.

978-1-61284-651-4/11/$26.00 ©2011 IEEE

of the techniques that we used to treat the bulk materials shown in Fig. 1 [17, 18]. In Section III, we present the scaling laws for the thin film contact resistance for the model shown in Fig. 2.

Thus, the results presented in this paper represent a vast generalization of the conventional theory for bulk contacts and thin film contacts.

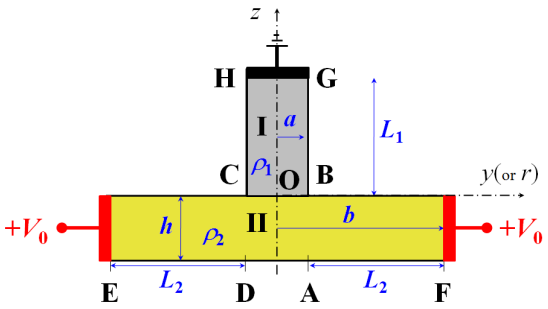

Figure 2. Thin film structures in either Cartesian or cylindrical geometries. Terminals *E* and *F* are held at a constant voltage (V_0) relative to terminal *GH*, which is grounded. The z-axis is the axis of rotation for the cylindrical geometry. The resistivity ratio ρ_1/ρ_2 in Regions I and II is arbitrary.

II. Contact Resistance of Bulk Contacts

Figure 1 shows the geometry of a generalized *a*-spot, Region I, which has a finite axial length 2*h*, joining two conducting current channels (II, III). This figure shows a Cartesian (cylindrical) composite current channel with half channel width (radius) of *a*, *b* and *c* ($a \le b$, $a \le c$), and electrical resistivity ρ_1, ρ_2 and ρ_3. It is assumed that the axial extents of channels II and III are so long that the current flow in these channels is uniform far from the contact region, I. The contact resistance was derived from series expansion of the solutions in different regions, and by matching the boundary condition at the interfaces.

A. Generalized Cartesian a-spot

For the Cartesian channel of Fig. 1, the scaling law for the total electrical resistance in Regions II, I, and III, including the interfaces of these regions for arbitrary values of *a, b, c, h*, ρ_1, ρ_2 and ρ_3 reads [11],

$$R = \frac{\rho_2 L_2}{2b\times W} + \frac{\rho_2}{4\pi W}\overline{R}_c\left(\frac{b}{a},\frac{\rho_1}{\rho_2}\right) + \frac{\rho_1\times 2h}{2a\times W} + \frac{\rho_3}{4\pi W}\overline{R}_c\left(\frac{c}{a},\frac{\rho_1}{\rho_3}\right) + \frac{\rho_3 L_3}{2c\times W}, \qquad \textbf{(Cartesian)} \quad (2)$$

where *W* denotes the channel width in the third, ignorable dimension that is perpendicular to the paper, and the rest of the symbols have been defined in Fig. 1. Equation (2) was synthesized from a vast amount of data. In Eq. (2), the first, third, and fifth term represents the bulk resistance in Regions II, I, and III, respectively. The second and the fourth term represent the interface (contact) resistances between Regions I and II, and between Regions I and III, respectively. In Eq. (2), $\overline{R}_c$ is approximately given by [11],

$$\overline{R}_c\left(\frac{b}{a},\frac{\rho_1}{\rho_2}\right) \cong \overline{R}_{c0}\left(\frac{b}{a}\right)\Big|_{LTZ} + 0.2274\times\left(\frac{2\rho_1}{\rho_1+\rho_2}\right)\times g\left(\frac{b}{a}\right), \quad (3)$$

$$\overline{R}_{c0}(b/a)\big|_{LTZ} = 4\ln(2b/\pi a) + 4\ln(\pi/2)\times f(b/a),$$
$$f(b/a) = 0 - 0.03250(a/b) + 1.06568(a/b)^2 - 0.24829(a/b)^3 + 0.21511(a/b)^4,$$
$$g(b/a) = 1 - 1.2281(a/b)^2 + 0.1223(a/b)^4 - 0.2711(a/b)^6 + 0.3769(a/b)^8, \quad (4)$$

where $\overline{R}_{c0}(x)\big|_{LTZ}$ is the normalized contact resistance of the Cartesian "*a*-spot" derived by Lau, Tang, and Zhang [11] for the special case in Fig. 1: $h = 0$, $b = c$, and $\rho_2 = \rho_3$. It is the Timsit analog for the Cartesian channel [cf. Eq. (7)]. Note that in Eq. (4), $f(1) = 1, f(\infty) = 0$, $g(1) = 0$, $g(\infty) = 1$, $\overline{R}_{c0}(1) = 0$, and $d\left[\overline{R}_{c0}(x)\big|_{LTZ}\right]/dx = 0$ when $x = b/a = 1$. Thus, from Eq. (3), the normalized interface resistance $\overline{R}_c(1,\rho_1/\rho_2) = 0$, as expected of Fig. 1 in the limit $b/a = 1$.

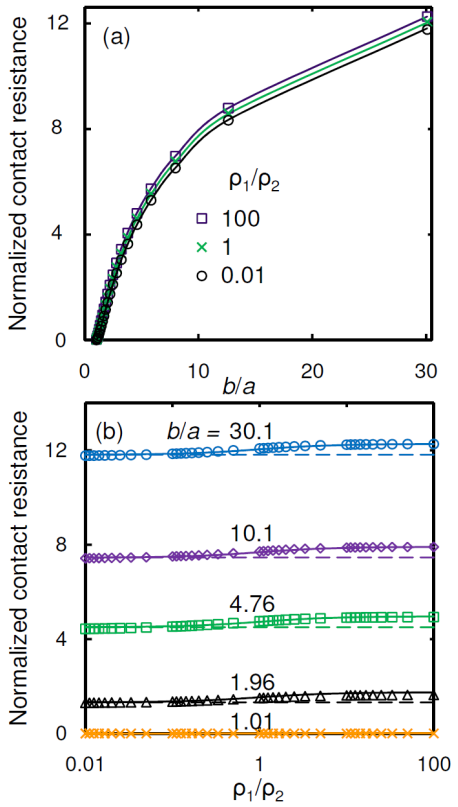

Figure 3. $\overline{R}_c(b/a,\rho_1/\rho_2)$ for semi-infinite Cartesian current channels, I and II, as a function of (a) aspect ratio *b*/*a*, and (b) resistivity ratio ρ_1/ρ_2; symbols for the exact theory, solid lines for the scaling law Eq. (3), and the dashed lines in (b) for the Cartesian *a*-spot theory ($\overline{R}_{c0}(b/a)\big|_{LTZ}$, Eq. (4)).

In the case of Cartesian semi-infinite channel ($L_2 >> b$, $h >> a$; Fig. 1), the interface resistance at $z = 0$, $\bar{R}_c(b/a, \rho_1/\rho_2)$, has an exact expression. This exact expression is well represented by the scaling law, Eq. (3), essentially for the entire range of $0 < \rho_1/\rho_2 < \infty$ and $b/a \geq 1$, as shown in Fig. 3. It is clear from Fig. 3(a) that $\bar{R}_c$ increases as b/a increases, for a given ρ_1/ρ_2. However, for a very broad range of ρ_1/ρ_2 from 10^{-2} to 10^2, $\bar{R}_c$ varies at the most by a difference of 0.4548 for a given aspect ratio b/a, as is evident in Fig. 3 (b).

The validity of the scaling law of Eq. (2) for Fig. 1 is further established by our demonstration that these scaling laws are indeed an excellent approximation in several known limiting cases [11]. The scaling law of Eq. (2) introduces an error of at most 10 percent in the normalized contact resistance ($\bar{R}_c$) in the worst case, $h = 0$ [11], as the interface resistance $\bar{R}_c(b/a, \rho_1/\rho_2)$ was derived under the assumption $h >> a$.

B. Generalized Cylindrical a-spot

For the cylindrical channel of Fig. 1, the scaling law for the total electrical resistance in Regions II, I, and III, including the interfaces of these regions for arbitrary values of *a, b, c, h*, ρ_1, ρ_2 and ρ_3 reads [11],

$$R = \frac{\rho_2 L_2}{\pi b^2} + \frac{\rho_2}{4a}\bar{R}_c\left(\frac{b}{a}, \frac{\rho_1}{\rho_2}\right) + \frac{\rho_1 \times 2h}{\pi a^2} \quad \textbf{(Cylindrical)} \qquad (5)$$
$$+ \frac{\rho_3}{4a}\bar{R}_c\left(\frac{c}{a}, \frac{\rho_1}{\rho_3}\right) + \frac{\rho_3 L_3}{\pi c^2},$$

where the symbols have been defined in Fig. 1. Equation (5) was synthesized from a vast amount of data. In Eq. (5), the first, third, and fifth term represents the bulk resistance in Regions II, I, and III, respectively. The second and the fourth term represent the interface (contact) resistances between Regions I and II, and between Regions I and III, respectively. In Eq. (5), $\bar{R}_c$ is approximately given by [11],

$$\bar{R}_c\left(\frac{b}{a}, \frac{\rho_1}{\rho_2}\right) \cong \bar{R}_{c0}\left(\frac{b}{a}\right)\Big|_{Timsit} + \frac{\Delta}{2} \times \left(\frac{2\rho_1}{\rho_1 + \rho_2}\right) \times g\left(\frac{b}{a}\right), \qquad (6)$$

$$\bar{R}_{c0}(b/a)\Big|_{Timsit} = 1 - 1.41581(a/b) + 0.06322(a/b)^2$$
$$+ 0.15261(a/b)^3 + 0.19998(a/b)^4, \qquad (7)$$
$$g(b/a) = 1 - 0.3243(a/b)^2 - 0.6124(a/b)^4$$
$$- 1.3594(a/b)^6 + 1.2961(a/b)^8,$$

where $\Delta = 32/3\pi^2 - 1 = 0.08076$ and $\bar{R}_{c0}(x)\big|_{\text{Timsit}}$ is the normalized contact resistance of the *a*-spot derived by Timsit and Rosenfeld [7, 8] for the special case in Fig. 1: $h = 0$, $b = c$, and $\rho_2 = \rho_3$. Both $g(x)$ and $\bar{R}_{c0}(x)\big|_{Timsit}$ are monotonically increasing functions of $x = b/a$ with $g(1) = 0$, $g(\infty) = 1$, $\bar{R}_{c0}(1)\big|_{Timsit} = 0$, $\bar{R}_{c0}(\infty)\big|_{Timsit} = 1$, and therefore Eq. (6) yields $\bar{R}_c(1, \rho_1/\rho_2) = 0$, as expected of the interface resistance from Fig. 1 in the limit $b/a = 1$.

In the case of cylindrical semi-infinite channel ($L_2 >> b$, $h >> a$; Fig. 1), the interface resistance at $z = 0$, $\bar{R}_c(b/a, \rho_1/\rho_2)$, has an exact expression. This exact expression is well represented by the scaling law, Eq. (6), essentially for the entire range of $0 < \rho_1/\rho_2 < \infty$ and $b/a \geq 1$, as shown in Fig. 4. It is clear from Fig. 4(a) that $\bar{R}_c$ increases as b/a increases, for a given ρ_1/ρ_2. Again, similar to the Cartesian case, for a very broad range of ρ_1/ρ_2 from 10^{-2} to 10^2, $\bar{R}_c$ varies only by a difference of $\Delta \cong 0.08076$ for a given aspect ratio b/a, as is evident in Fig. 4(b).

The validity of the scaling law of Eq. (5) for Fig. 1 is further established by our demonstration that these scaling laws are indeed an excellent approximation in several known limiting cases [11]. Like the Cartesian channel, the scaling law of Eq. (5) introduces an error of at most 10 percent in the normalized contact resistance ($\bar{R}_c$) in the worst case, $h = 0$ [11], as Eq. (5) was derived for $h >> a$.

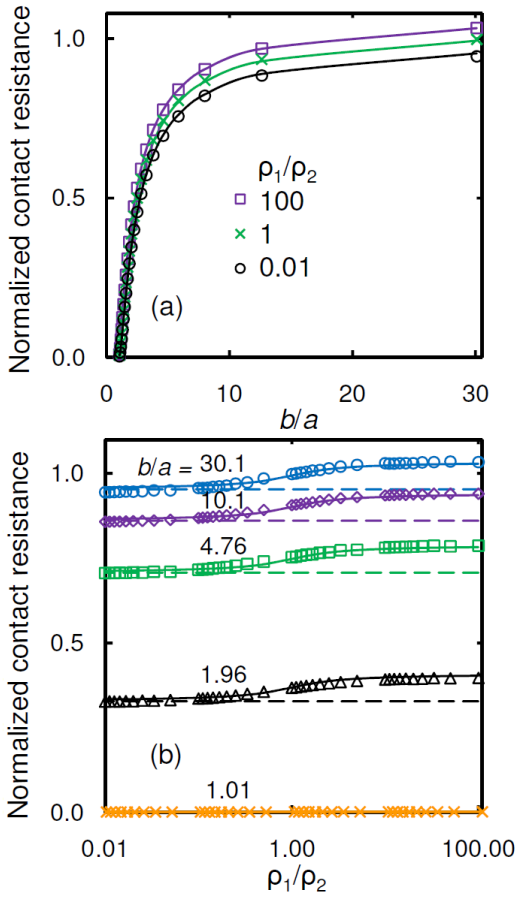

Figure 4. $\bar{R}_c(b/a, \rho_1/\rho_2)$ for semi-infinite cylindrical current channels, I and II, as a function of (a) aspect ratio b/a, and (b) resistivity ratio ρ_1/ρ_2; symbols for the exact theory, solid lines for the scaling law Eq. (6), and the dashed lines in (b) for the cylindrical *a*-spot theory ($\bar{R}_{c0}(b/a)\big|_{Timsit}$, Eq. (7)).

III. CONTACT RESISTANCE OF THIN FILM CONTACTS

The models of contact resistance in Section II are inapplicable to the thin film contact geometry shown in Fig. 2. This is particularly the case when the current is mostly confined to the immediate vicinity of the constriction and flows parallel to the thin film boundary. Figure 2 shows both Cartesian and cylindrical geometries of the thin film. In Cartesian (cylindrical) geometry, the current flows inside the base thin film with width (thickness) h and electrical resistivity ρ_2, converging towards the center of the joint region, and feeds into the top channel with half-width (radius) a and electrical resistivity ρ_1.

A. Cartesian Thin Film Contact

For the Cartesian geometry of Fig. 2, the total resistance, R, from EF to GH is found to be [18],

$$R = \frac{\rho_2 L_2}{2h\times W} + \frac{\rho_2}{4\pi W}\overline{R}_c\left(\frac{a}{b},\frac{a}{h},\frac{\rho_1}{\rho_2}\right) + \frac{\rho_1 L_1}{2a\times W}, \quad \textbf{(Cartesian)}\ (8)$$

where W denotes the channel width in the third, ignorable dimension that is perpendicular to the paper, and the rest of the symbols have been defined in Fig. 2. In Eq. (8), the first term represents the bulk resistance of the thin film base, from A to F, and from D to E, where $L_2 = b - a$. The third term represents the bulk resistance of the top region from B to G. The second term represents the remaining constriction (or contact) resistance, R_c, for the region $ABCD$ [17, 18]. The *exact* expression for $\overline{R}_c$ is derived by using Fourier series representation for the potentials in Region I and Region II, and then matching the boundary conditions at the interface, BC [18]. From the exact theory, it is found that $\overline{R}_c$ becomes almost a constant if either $L_2/a >> 1$ or $L_2/h >> 1$, in which case $\overline{R}_c$ is determined only by the value of a/h and ρ_1/ρ_2, independent of b [17, 18]. The vast amount of data collected from the exact calculations allows us to synthesize a simple scaling law for the normalized contact resistance $\overline{R}_c$ in Eq. (8) as [18],

$$\overline{R}_c\left(\frac{a}{h},\frac{\rho_1}{\rho_2}\right) \cong \overline{R}_{c0}\left(\frac{a}{h}\right) + \frac{\Delta\left(\frac{a}{h}\right)}{2}\times\frac{2\rho_1}{\rho_1+\beta\left(\frac{a}{h}\right)\rho_2}, \qquad (9)$$

$$\overline{R}_{c0}(a/h) = \overline{R}_c(a/h)\big|_{\rho_1/\rho_2\to 0} = 2\pi a/h - 4\ln\left[\sinh(\pi a/2h)\right], \qquad (10)$$

$$\Delta(a/h) = \begin{cases} 0.5346(a/h)^2 + 0.0127(a/h) + 0.4548, \\ \qquad 0.03 \le a/h \le 1; \\ 0.0147x^6 - 0.0355x^5 + 0.1479x^4 \\ +0.4193x^3 + 1.1163x^2 + 0.9970x + 1, \\ \qquad x = \ln(a/h), 1 < a/h \le 30, \end{cases} \qquad (11)$$

$$\beta(a/h) = -0.0003(a/h)^2 + 0.1649(a/h) + 0.6727, \quad 0.03 \le a/h \le 30.$$

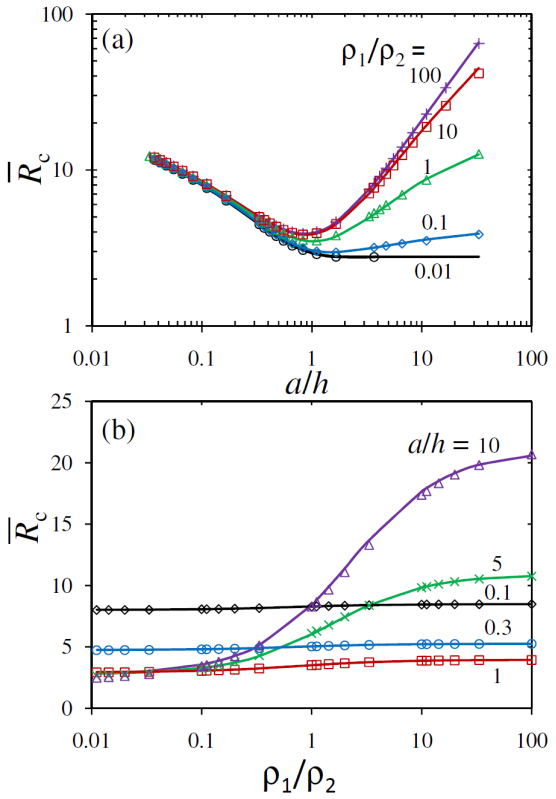

Figure 5. $\overline{R}_c(a/h, \rho_1/\rho_2)$ for Cartesian thin film structures in Fig. 2, as a function of (a) aspect ratio a/h, and (b) resistivity ratio ρ_1/ρ_2; symbols for the exact theory, solid lines for the scaling law Eq. (9).

The scaling law of Cartesian thin film contact resistance, Eq. (9), is shown in Fig. 5, which compares extremely well with the exact theory, for the range of $0 < \rho_1/\rho_2 < \infty$ and $0.03 \le a/h \le 30$. (We have not found the scaling law for $a/h > 30$ for general values of ρ_1/ρ_2, as data for $a/h > 30$ are not easy to generate from the exact theory [18].) Each data point (symbol) in Fig. 5 consists of many combinations of b/a and b/h, with either $L_2 >> a$ *or* $L_2 >> h$. Again, $\overline{R}_c$ is independent of b, provided either $L_2 >> a$ or $L_2 >> h$. It is clear that there is a minimum value of $\overline{R}_c$ in the region of a/h near unity, for a given ρ_1/ρ_2. This a/h value for minimum $\overline{R}_c$ decreases slightly as ρ_1/ρ_2 increases. For the special case of $\rho_1/\rho_2 = 1$, the minimum $\overline{R}_c = 2\pi - 4\ln 2 = 3.5106$ occurs exactly at $a/h = 1$ [16, 17], and if a/h deviates from 1, $\overline{R}_c$ increases logarithmically as $\overline{R}_c \cong -4\ln(a/h) - 1.5452$ for $a/h << 1$, and $\overline{R}_c \cong 4\ln(a/h) - 1.5452$ for $a/h >> 1$ [16, 17]. In the regime $a/h < 1$, the range of variation $\overline{R}_c(\rho_1/\rho_2)$ for a given a/h is insignificant (Fig. 5 (a)); however, in the regime of $a/h > 1$, $\overline{R}_c(\rho_1/\rho_2)$ for a given a/h may change by an order of magnitude or more. Once more we have not established the asymptotic dependence of $\overline{R}_c$ as $a/h \to \infty$.

B. Cylindrical Thin Film Contact

For the cylindrical geometry of Fig. 2, the total resistance, R, from EF to GH is found to be [18],

$$R=\frac{\rho_2}{2\pi h}\ln\left(\frac{b}{a}\right)+\frac{\rho_2}{4a}\overline{R}_c\left(\frac{a}{b},\frac{a}{h},\frac{\rho_1}{\rho_2}\right)+\frac{\rho_1 L_1}{\pi a^2}. \textbf{(Cylindrical)} \quad (12)$$

where the symbols have been defined in Fig. 2. In Eq. (12), the first term represents the bulk resistance of the thin film base, from A to F, and from D to E [12, 17]. The third term represents the bulk resistance of the top region from B to G. The second term represents the remaining constriction (or contact) resistance, R_c, for the region $ABCD$ [18]. The *exact* expression for $\overline{R}_c$ is derived by using Fourier series representation for the potentials in Region I and Region II, and then matching the boundary conditions at the interface, BC [18]. Similar to the Cartesian case, from the exact theory, it is found that $\overline{R}_c$ becomes almost a constant if either $L_2/a >> 1$ or $L_2/h >> 1$, in which case $\overline{R}_c$ is determined only by the value of a/h and ρ_1/ρ_2, independent of b. The vast amount of data collected from the exact calculations allows us to synthesize a simple scaling law for the normalized contact resistance in Eq. (12) as [18],

$$\overline{R}_c\left(\frac{a}{h},\frac{\rho_1}{\rho_2}\right)\cong\overline{R}_{c0}\left(\frac{a}{h}\right)+\frac{\Delta\left(\frac{a}{h}\right)}{2}\times\frac{2\rho_1}{\rho_1+\beta\left(\frac{a}{h}\right)\rho_2}, \quad (13)$$

$$\overline{R}_{c0}(a/h)=\overline{R}_c(a/h)\big|_{\rho_1/\rho_2\to 0}$$

$$=\begin{cases}1-2.2968(a/h)+4.9412(a/h)^2-6.1773(a/h)^3\\ +3.811(a/h)^4-0.8836(a/h)^5, \quad 0.001\le a/h\le 1;\\ 0.295+0.037(h/a)+0.0595(h/a)^2, \quad 1<a/h<10,\end{cases} \quad (14)$$

$$\Delta(a/h)=\begin{cases}0.0184(a/h)^2+0.0073(a/h)+0.0808,\\ \qquad 0.001\le a/h\le 1;\\ 0.0409x^4-0.1015x^3+0.265x^2-0.0405x\\ +0.1065, \qquad x=\ln(a/h), 1<a/h<10,\end{cases}$$

$$\beta(a/h)=0.0016(a/h)^2+0.0949(a/h)+0.6983,$$
$$0.001\le a/h<10. \quad (15)$$

The scaling law of cylindrical thin film contact resistance, Eq. (13), is shown in Fig. 6, which compares very well with the exact theory, for the range of $0<\rho_1/\rho_2<\infty$ and $0.001\le a/h<10$. (We have not found the scaling law for $a/h>10$.) Each data point (symbol) in Fig. 6 consists of many combinations of b/a and b/h, with either $L_2 >> a$ *or* $L_2 >> h$. Again, $\overline{R}_c$ is independent of b, provided either $L_2 >> a$ or $L_2 >> h$. For a given a/h, $\overline{R}_c$ increases as ρ_1/ρ_2 increases, similar to the Cartesian case. It is clear that there is a minimum value of $\overline{R}_c$ in the region of a/h near 1.5, for a given ρ_1/ρ_2. The a/h value for minimum $\overline{R}_c$ decreases slightly as ρ_1/ρ_2 increases. For the special case of $\rho_1/\rho_2 = 1$, the minimum $\overline{R}_c\cong 0.42$ occurs at $a/h\cong 1.6$ [17]. In the regime $a/h < 1$, the variation $\overline{R}_c(\rho_1/\rho_2)$ for a given a/h is insignificant; however, in the regime of $a/h > 1$, $\overline{R}_c(\rho_1/\rho_2)$ for a given a/h changes by a factor in the single digits, up to an order of magnitude as shown in Fig. 6 (a). The cylindrical case differs from the Cartesian case in one aspect, namely, as $a/h\to 0$, $\overline{R}_c$ converges to constant values, ranging from about 1 to 1.08, essentially for $0<\rho_1/\rho_2<\infty$. The explanation follows. If $a/h\to 0$, both the radius and thickness of the film region are much larger than the radius a of the top cylinder (Fig. 2), as if two semi-infinite long cylinders are joining together with radius ratio of $b/a\to\infty$. In this case, the a-spot [6] theory gives a value of $\overline{R}_c$ in the range of 1 to 1.08, for $0<\rho_1/\rho_2<\infty$ [c.f. Eq. (2) of Ref. 11]. Once more, we have not established the asymptotic dependence of $\overline{R}_c$ as $a/h\to\infty$.

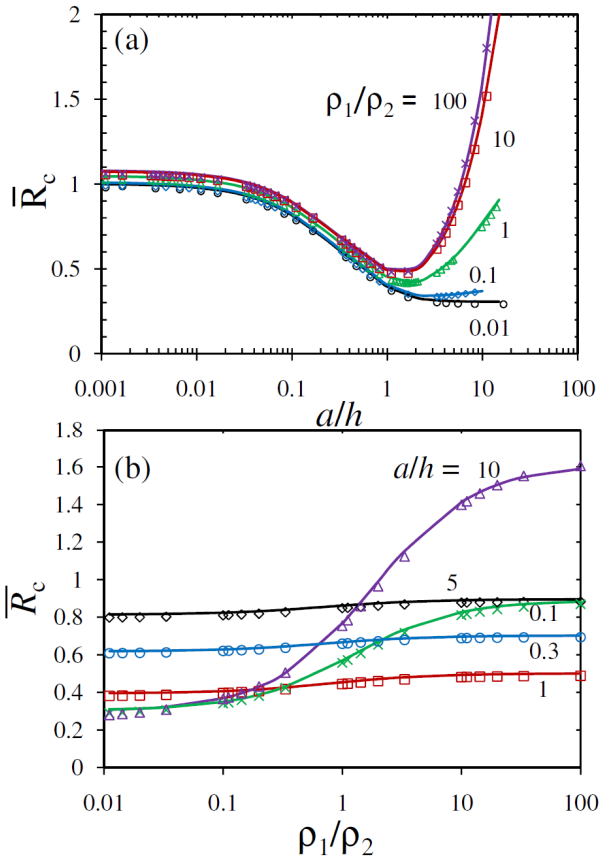

Figure 6. $\overline{R}_c(a/h,\rho_1/\rho_2)$ for cylindrical thin film structures in Fig. 2, as a function of (a) aspect ratio a/h, and (b) resistivity ratio ρ_1/ρ_2; symbols for the exact theory, solid lines for the scaling law Eq. (13).

IV. SUMMARY

In this paper, we presented simple, accurate, analytical scaling laws of contact resistance with dissimilar materials for both bulk contacts (Fig. 1) and thin film contacts (Fig. 2), over a very large range of geometries and resistivities. Both Cartesian and cylindrical geometries are analyzed.

The bulk contact (Fig. 1) is a substantial generalization of Holm's *a*-spot, with a finite contact region, I, and with arbitrary values of *a, b, c, h*, ρ_1, ρ_2 and ρ_3. The explicit scaling law presented here provides the building block for the contact resistance of a single asperity to allow a statistical treatment for a contacting, rough, surface. Based on our calculations, we found that if the electrical contact (Region I) is highly resistive ($\rho_1 >> \rho_2, \rho_1 >> \rho_3$), then the bulk resistance (the third term on the RHS of Eqs. (2) and (5)) dominates over the interface resistance (the second and fourth term on the RHS of Eqs. (2) and (5)) once the contact region's axial length ($2h$) exceeds a few times $(\rho_2/\rho_1)a$ and $(\rho_3/\rho_1)a$. Once the geometry (a,b,c,h) is specified, the interface resistance depends mainly on the electrical resistivity of the main channel (ρ_2, ρ_3); it is insensitive to the resistivity of the contact region (ρ_1).

The scaling laws of the contact resistance of thin film contact (Fig. 2) are also established, for the range $0 < \rho_1/\rho_2 < \infty$, and $0.03 \le a/h \le 30$ for the Cartesian case, and $0.001 \le a/h < 10$ for the cylindrical case. It is found that, at a given resistivity ratio, the thin film contact resistance primarily depends on the ratio of constriction size (a) to the film thickness (h) only, as long as either $L_2 >> a$ or $L_2 >> h$. In the latter cases, the electrostatic fringe field is restricted to the constriction corner only, and becomes insensitive to the location of terminals for the thin film region. If the constriction size (a) is small compared with film thickness (h), the thin film contact resistance is insensitive to the resistivity ratio. However, if $a/h > 1$, the contact resistance varies significantly with the resistivity ratio. Typically, the minimum contact resistance is realized with $a/h \sim 1$, for both Cartesian and cylindrical thin films.

Our analysis here may readily be adapted to thermal conduction in various bulk and thin film structures under steady state. It could also be applicable to the maximization of channel flows at a given pressure.

REFERENCES

[1] M. R. Gomez, J. C. Zier, R. M. Gilgenbach, D. M. French, W. Tang, and Y. Y. Lau, "Effect of soft metal gasket contacts on contact resistance, energy deposition, and plasma expansion profile in a wire array Z pinch", *Rev. Sci. Instrum.* vol 79, p. 093512, 2008.

[2] R. M. Gilgenbach, Y. Y. Lau, H. McDowell, K. L. Cartwright, and T. A. Spencer, "Crossed-Field Devices", in *Modern Microwave and Millimeter Wave Power Electronics*, Chap. 6, edited by R.J. Barker, N.C. Luhmann, J.H. Booske, and G.S. Nusinovich, IEEE Press, Piscataway, NJ 2004.

[3] N. M. Jordan, Y. Y. Lau, David M. French, R. M. Gilgenbach, and P. Pengvanich, "Electric field and electron orbits near a triple point", *J. Appl. Phys*. vol 102, p. 033301, 2007.

[4] R. Miller, Y. Y. Lau, and John H. Booske, "Electric field distribution on knife-edge field emitters", *Appl. Phys. Lett.* vol 91, p. 074105, 2007.

[5] P. Zhang, Y. Y. Lau, and R. M. Gilgenbach, "Analysis of radio-frequency absorption and electric and magnetic field enhancements due to surface roughness", *J. Appl. Phys*. vol 105, p. 114908, 2009.

[6] R. Holm, *Electric Contact*, Springer-Verlag, Berlin, ed. 4, 1967.

[7] A. M. Rosenfeld and R. S. Timsit, "The potential distribution in a constricted cylinder: An exact solution," *Quart Appl. Math.*, vol. 39, p. 405, 1981.

[8] R. S. Timsit, "Electrical contact resistance: properties of stationary interfaces", *IEEE Trans. Compon. Packag. Technol*. vol 22, p. 85, 1999.

[9] Y. Y. Lau and Wilkin Tang, "A higher dimensional theory of electrical contact resistance", *J. Appl. Phys.* vol 105, p. 124902, 2009.

[10] M. R. Gomez, D. M. French, W. Tang, P. Zhang, Y. Y. Lau, and R. M. Gilgenbach, "Experimental validation of a higher dimensional theory of electrical contact resistance", *Appl. Phys. Lett.* vol 95, p. 072103, 2009.

[11] P. Zhang and Y. Y. Lau, "Scaling Laws for Electrical Contact Resistance with Dissimilar Materials", *J. Appl. Phys.* vol. 108, p. 044914, 2010. There was a typo in this paper. In Eq. (6) of this paper, the term $-2.2281(a/b)^2$ in $g(b/a)$ should read $-1.2281(a/b)^2$.

[12] R. Timsit, "Constriction resistance of thin-film contacts," Electrical Contacts, Processdings of the 54th IEEE Holm Conference on, pp. 332-336, Oct. 2008.

[13] M. B. Read, J. H. Lang, A. H. Slocum, and R. Martens, "Contact Resistance in Flat Thin Films", Electrical Contacts, Proceedings of the 55th IEEE Holm Conference on, pp. 303 – 309, 2009.

[14] G. Norberg, S. Dejanovic, H. Hesselbom, "Contact resistance of thin metal film contacts," Components and Packaging Technologies, IEEE Transactions on, vol. 29, No. 2, pp. 371–378, 2006.

[15] P. M. Hall, "Resistance calculations for thin film patterns", *Thin Solid Films* vol 1, p. 277, 1967.

[16] P. M. Hall, "Resistance calculations for thin film rectangles", *Thin* Solid Films vol 300, p. 256, 1997.

[17] P. Zhang, Y. Y. Lau, and R. M. Gilgenbach, "Minimization of thin film contact resistance", *Appl. Phys. Lett.* vol 97, p. 204103, 2010.

[18] P. Zhang, Y. Y. Lau, and R. M. Gilgenbach, "Thin film contact resistance with dissimilar materials", *J. Appl. Phys.* (in the press, 2011).